Available online at www.sciencedirect.com
SCIENCE DIRECT®
Journal of Solid State Chemistry 178 (2005) 200–206
JOURNAL OF SOLID STATE CHEMISTRY
www.elsevier.com/locate/jssc

The crystal growth and magnetic properties of Ln_2LiIrO_6 (Ln = La, Pr, Nd, Sm, Eu)

Samuel J. Mugavero III, Mark D. Smith, Hans-Conrad zur Loye*

Department of Chemistry and Biochemistry, University of South Carolina, 631 Sumter Street, GSRC 531, Columbia, SC 29208, USA

Received 1 July 2004; received in revised form 14 October 2004; accepted 22 October 2004

Abstract

Single crystals of a series of lanthanide lithium iridium oxides, Ln_2LiIrO_6 (Ln = La, Pr, Nd, Sm, Eu) with the double perovskite structure have been grown from molten LiOH/KOH fluxes. The compounds crystallize in a distorted 1:1 rock salt lattice of Li^+ and Ir^{5+} cations in the monoclinic space group $P2_1/n$. The magnetic susceptibilities of Ln_2LiIrO_6 (Ln = Pr, Nd, Sm, Eu) are presented.

Keywords: Crystal growth; Double perovskite; Hydroxide flux; Crystal structure; Magnetic properties; La_2LiIrO_6; Pr_2LiIrO_6; Nd_2LiIrO_6; Sm_2LiIrO_6; Eu_2LiIrO_6

1. Introduction

Perovskite oxides are perhaps the most studied family of compounds in solid-state chemistry due to their inherent ability to accommodate a wide range of elemental compositions and to display a wealth of structural variations. In particular, their extensive compositional flexibility is of interest as it enables these structures to accommodate almost every element of the periodic table. In its ideal form, the cubic perovskite, ABO_3, consists of corner-sharing BO_6 octahedra with the A-cation occupying the 12-fold coordination site formed in the middle of a cube of eight such octahedra. The ideal double perovskite structure of the general formula $A_2BB'O_6$ is obtained when the B cation is substituted by a B' cation in an ordered 1:1 fashion, doubling the unit cell, Fig. 1. This arrangement determines the crystal system and together, with the composition, determine the physical properties of the double perovskite.

Among the double perovskites, compounds that contain Ir(V) have been investigated extensively owing to the wide variety of potential compositions. When one considers the general formula $AA'BIr5^+O_6$, Ir(V) may be stabilized with A and A' representing an alkaline earth and B a trivalent cation as in Ba_2LaIrO_6 [1]. Additionally, A could represent an alkaline earth and A' a lanthanide cation with B being a divalent cation as exemplified by $BaLaCoIrO_6$ [2]. Finally, it is also possible to have A and A' represent a lanthanide and B an alkali metal, exemplified by the composition La_2NaIrO_6 [3] and Ln_2LiIrO_6 (Ln = La, Pr, Nd, Sm, Eu) the title compounds of this paper.

Recently, our group has focused on the single crystal growth of lanthanide containing oxides of platinum group metals in an effort to investigate both the structural chemistry and the magnetic properties of such compounds. In order to do so, we developed an effective synthetic approach employing molten hydroxide fluxes. The acid–base chemistry of hydroxide fluxes, described by the Lux–Flood acid–base definition, allows for a wide range of species to be present in solution, an essential prerequisite for their incorporation into single crystals. It is known that molten hydroxides are an excellent solvent of crystallization for lanthanide containing oxides, where the solubility of the lanthanides is dictated by the acid–base properties of the melt.

*Corresponding author. Fax: +803 777 8505.
E-mail address: zurloye@mail.chem.sc.edu (H.-C. zur Loye).

0022-4596/$ - see front matter © 2004 Elsevier Inc. All rights reserved.
doi:10.1016/j.jssc.2004.10.033

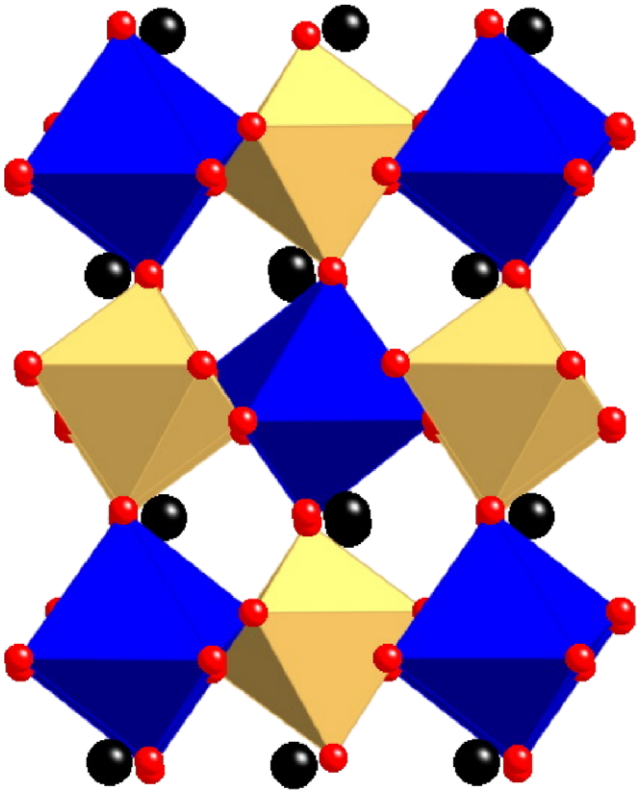

Fig. 1. Crystal structure of Ln_2LiIrO_6 viewed down [100] (*a*-axis). The IrO_6 octahedra are shown in black, LiO_6 octahedra are gray, the *Ln* atoms are represented by large light gray spheres, and the O atoms are the small dark gray spheres.

Specifically, the water content of the melt must be controlled to enable the dissolution of the lanthanide oxides (Ln_2O_3's), which are only soluble in acidic "wet" melts. We have recently shown that such "wet" melts are one route for the growth of oxide single crystals containing both lanthanide and platinum group metals [3–6].

We recently reported the growth of single crystals of the formula Ln_2NaIrO_6 (*Ln* = La, Pr, Nd), where we were unable to prepare members of this series containing lanthanides smaller than neodymium [3]. It appeared that for this series a Goldschmidt tolerance factor of approximately 0.86 represented the lower limit of stability. The substitution of the smaller lithium cation for sodium in this structure, however, results in a larger tolerance factor and, hence, one would predict that it should be possible to synthesize compounds containing rare earths smaller than neodymium for the series Ln_2LiIrO_6. This prediction turned out to be correct and herein we present the crystal growth, structure determination, and magnetic properties of the series of double perovskites Ln_2LiIrO_6 (*Ln* = La, Pr, Nd, Sm, Eu).

2. Experimental

2.1. Crystal growth and polycrystalline preparation

Crystals of La_2LiIrO_6, Pr_2LiIrO_6, Nd_2LiIrO_6, Sm_2LiIrO_6, and Eu_2LiIrO_6 were grown from "acidic" high temperature hydroxide melts. The alkali earth hydroxides used typically contain 15% water by weight. La_2O_3 (Alfa Aesar 99.9%, 0.75 mmol) or Pr_2O_3 (Cerac, 99.9%, 0.75 mmol) or Nd_2O_3 (Johnson Matthey, 99.9%, 0.75 mmol) or Sm_2O_3 (Alfa Aesar, 99.9%, 0.75 mmol) or Eu_2O_3 (Avocado, 99.9%, 0.75 mmol), Ir (Engelhard, 99.9%, 0.5 mmol), LiOH (Alfa Aesar, 98%, 2.0 g), and KOH (Fisher, ACS reagent, 2.0 g) were loaded into silver tubes that had been previously flame sealed at one end. The tops of the tubes were crimped, and folded three times before being placed upright into a programmable box furnace. The tubes were heated to 700 °C in one hour, held at that temperature for 24 h (36 h for Nd_2LiIrO_6 and Eu_2LiIrO_6) and then cooled to room temperature by shutting off the furnace. The crystals were removed from the flux matrix by dissolving the flux in methanol (the lithium containing crystals are water sensitive and, hence, water should not be used to dissolve the flux) and isolating the crystals by vacuum filtration.

Polycrystalline samples of Pr_2LiIrO_6 and Nd_2LiIrO_6 were prepared for use in magnetic measurements by grinding stoichiometric amounts of Pr_2O_3 (Cerac, 99.9%, 1 mmol) or Nd_2O_3 (Johnson Matthey, 99.9%, 1 mmol), Ir (Engelhard, 99.9%, 1 mmol), and Li_2CO_3 (Johnson Matthey, 99.999%, 0.5 mmol plus 10% excess by weight) in an agate mortar and pestle and then heating the powder under flowing oxygen. The samples were heated at a rate of 15 °C/min to 850–1050 °C for a total of 96 h. Reaction progress was monitored by powder X-ray diffraction patterns after each 24 h heating interval. Reactions were deemed complete after successive powder patterns were unchanged. Phase purity was established by Rietveld refinement of the data using the atomic positions from the single crystal structure solution. Polycrystalline samples of Sm_2LiIrO_6 and Eu_2LiIrO_6 could not be prepared as homogeneous phases and hence handpicked single crystals of these phases were used for magnetic measurements.

2.2. Scanning electron microscopy

Crystals were analyzed by scanning electron microscopy using an FEI Quanta SEM instrument utilized in the low vacuum mode. Energy dispersive spectroscopy verified the presence of Ir, O and the respective lanthanide element, and within the detection limits of the instrument, confirmed the absence of extraneous elements, such as silver. The presence of Li was undetectable due to limitations of the instrument.

2.3. Structural determination

For the structure determination of Ln_2LiIrO_6 (Ln = La, Pr, Nd, Sm, Eu), X-ray intensity data were measured using black block crystals or cut sections of crystals, which were epoxied onto the end of a thin glass fiber and measured at 294 K on a Bruker SMART APEX CCD-based diffractometer system (Mo$K\alpha$ radiation, $\lambda = 0.71073$ Å) [7]. The raw data frames were integrated into reflection intensity files with the Bruker SAINT+ program [7], which also applied corrections for Lorentz and polarization effects. Analysis of the data showed negligible crystal decay during data collection. Empirical absorption corrections were applied with the program SADABS [7].

The title compounds adopt the monoclinic double perovskite structure type with space group $P2_1/n$. Positional and thermal parameters were refined by full-matrix least-squares against F^2 using the SHELXTL software package [8]. For the structure determination of Eu_2LiIrO_6, only the heavy metal atoms were refined with anisotropic displacement parameters and the lithium and oxygen atoms were refined isotropically. None of the compounds showed any significant deviation from unity occupancy during refinement of site occupation factors for the heavy atoms.

2.4. Magnetic susceptibility

The magnetic susceptibilities of polycrystalline powders of Pr_2LiIrO_6 and Nd_2LiIrO_6 and of loose crystals of Sm_2LiIrO_6, and Eu_2LiIrO_6 were measured using a Quantum Design MPMS XL SQUID magnetometer. Magnetic measurements were not performed for La_2LiIrO_6 as the magnetic properties have been previously published [9,10]. The samples were measured under both zero field cooled (ZFC) and field cooled (FC) conditions in applied fields of 1 and 10 kG over the temperature range of $2\,K \leqslant T \leqslant 300\,K$. The samples were contained in gel capsules suspended in a plastic straw for immersion into the SQUID. The small diamagnetic contribution of the gelatin capsule containing the sample had negligible contribution to the overall magnetization, which was dominated by the sample.

3. Results and discussion

3.1. Crystal structure

Hydroxide melts have proven to be an excellent medium for synthesizing lanthanide containing oxides [11] due to their acid–base properties that are best described by the Lux–Flood acid–base definition [12,13]. The application of the Lux–Flood description indicates the need for controlling the water content of the flux in order to control its acid–base properties and hence the solubility of the rare earths within it. It has been established that rare earth oxides (RE_2O_3) are soluble in acidic (“wet”) hydroxide solutions [11,14]. Single crystals of La_2LiIrO_6, Pr_2LiIrO_6, Nd_2LiIrO_6, Sm_2LiIrO_6, and Eu_2LiIrO_6 were grown in sealed silver tubes containing acidic molten hydroxide solutions. Since the tubes were sealed, the dehydration of the melt was minimized and a relative constant acidity of the melt over the course of the experiment was maintained.

La_2LiIrO_6, Pr_2LiIrO_6, Nd_2LiIrO_6, Sm_2LiIrO_6, and Eu_2LiIrO_6 crystallize in the space group $P2_1/n$, with the monoclinic-distorted double perovskite structure type [15]. La_2LiIrO_6 has been previously reported in the orthorhombic space group $Pmm2$ [9,10] based on powder diffraction data. Since the monoclinic distortion is very small in this compound, however (the β angle deviates from 90° by only 0.177°) it would be difficult to detect using X-ray powder diffraction. The $P2_1/n$ space group allows for a 1:1 ordered arrangement of the B and B' cations in a rock-salt type lattice and the tilting of the BO_6 and $B'O_6$ octahedra to accommodate the small size of the A cation. The Glazer tilt system assigned to the $P2_1/n$ space group is #10, $a-a-b+$ [16–18]. In the title compounds, the Li^+ and Ir^{5+} cations lie on the two crystallographically independent octahedral sites, while the Ln^{3+} cations occupy the A site in an 8-fold coordination environment. Relevant crystallographic data for the five materials are shown in Table 1, atomic positions are represented in Table 2, and selected interatomic distances and bond angles are listed in Table 3.

Iridium is most commonly found in the tetravalent oxidation state; however, the use of an oxygen atmosphere or a highly oxidizing media, such as molten hydroxide fluxes, makes it possible to stabilize oxidation states of +5 and +6 [19,20]. The Ir–O distances in Ln_2LiIrO_6 (Ln = La, Pr, Nd, Sm, Eu) are consistent with the observed values found in other Ir(V) oxides [1,10], thus supporting the pentavalent state of iridium in these oxides. The Li–O distances range from 2.035(5) Å in Nd_2LiIrO_6 to 2.152(10) Å in Eu_2LiIrO_6 and are typical for Li^+ in an octahedral oxide environment [21].

The double perovskite structure of the title compounds is distorted due to tilting of the MO_6 octahedra while maintaining their corner-sharing connectivity. This phenomenon is commonly observed for perovskites with smaller A-cations and, hence, Goldschmidt tolerance factors smaller than 1. The A–O bond lengths are limited to a narrow range and, therefore, the only means for the structure to accommodate smaller A-cations is by distorting the Li–O–Ir bond angle. From a geometric standpoint, a smaller A-cation results in a more distorted M–O–M angle (away from the ideal value of 180°), and consequently the β angle of a monoclinic unit

Table 1
Crystal data and structural refinement for La_2LiIrO_6, Pr_2LiIrO_6, Nd_2LiIrO_6, Sm_2LiIrO_6, Eu_2LiIrO_6

Empirical formula	La_2LiIrO_6	Pr_2LiIrO_6	Nd_2LiIrO_6	Sm_2LiIrO_6	Eu_2LiIrO_6
Formula weight ($g\,mol^{-1}$)	572.96	576.96	583.62	595.84	599.06
Space group	$P2_1/n$	$P2_1/n$	$P2_1/n$	$P2_1/n$	$P2_1/n$
Unit cell dimensions					
a (Å)	5.5536(3)	5.4593(3)	5.4290(2)	5.3736(3)	5.3549(5)
b (Å)	5.6355(3)	5.7219(3)	5.7412(2)	5.7480(4)	5.7538(5)
c (Å)	7.8528(4)	7.7350(4)	7.7040(3)	7.6346(5)	7.6129(7)
β (deg)	90.177(2)	90.222(2)	90.5430(10)	90.368(2)	90.782(3)
V (Å^3)	245.77(2)	241.62(2)	240.12(2)	235.81(3)	234.54(4)
Z	2	2	2	2	2
Density (calculated) ($g\,cm^{-3}$)	7.742	7.930	8.072	8.392	8.483
Absorption coefficient (mm^{-1})	44.023	47.262	48.891	52.668	54.658
$F(0\,0\,0)$	484	492	496	504	508
Crystal size (mm)	$0.04 \times 0.02 \times 0.02$	$0.08 \times 0.06 \times 0.04$	$0.04 \times 0.04 \times 0.03$	$0.04 \times 0.04 \times 0.03$	$0.02 \times 0.02 \times 0.01$
θ_{max} (deg)	35.62	34.94	35.06	32.62	28.29
Reflections collected	5143	4289	4409	3848	2561
Independent reflections	1123 ($R_{int} = 0.0494$)	1056 ($R_{int} = 0.0370$)	1065 ($R_{int} = 0.0367$)	852 ($R_{int} = 0.0342$)	584 ($R_{int} = 0.0578$)
Goodness-of-fit on F^2	1.066	1.234	1.087	1.267	1.088
R indices (all data)	$R_1 = 0.0470$, $wR_2 = 0.0844$	$R_1 = 0.0318$, $wR_2 = 0.0716$	$R_1 = 0.0278$, $wR_2 = 0.0587$	$R_1 = 0.0394$, $wR_2 = 0.0712$	$R_1 = 0.0450$, $wR_2 = 0.0705$
Largest diffraction peak and hole (e^- Å^{-3})	5.453 and –3.085	5.011 and –3.014	3.348 and –1.847	3.953 and –4.796	2.931 and –2.936

Table 2
Atomic coordinates and equivalent isotropic displacement parameters for La_2LiIrO_6, Pr_2LiIrO_6, Nd_2LiIrO_6, Sm_2LiIrO_6, Eu_2LiIrO_6, respectively

	x	y	z	U_{eq}
La_2LiIrO_6				
La	0.4908(1)	0.0456(1)	0.2508(1)	0.008(1)
Li	0	0	0	0.019(5)
Ir	1/2	1/2	0	0.005(1)
O1	0.2173(11)	0.2984(12)	0.0403(8)	0.007(1)
O2	0.5767(12)	0.4836(11)	0.2443(8)	0.008(1)
O3	0.3011(11)	0.7831(12)	0.0419(12)	0.008(1)
Pr_2LiIrO_6				
Pr	0.4861(1)	0.0628(1)	0.2511(1)	0.006(1)
Li	0	0	0	0.010
Ir	1/2	1/2	0	0.004(1)
O1	0.2064(12)	0.3115(12)	0.0449(8)	0.007(1)
O2	0.5903(11)	0.4740(11)	0.2453(9)	0.007(1)
O3	0.3154(11)	0.7870(12)	0.0485(8)	0.006(1)
Nd_2LiIrO_6				
Nd	0.4844(1)	0.0671(1)	0.2513(1)	0.006(1)
Li	0	0	0	0.014(3)
Ir	1/2	1/2	0	0.004(1)
O1	0.2031(8)	0.3118(8)	0.0467(6)	0.008(1)
O2	0.5937(8)	0.4723(7)	0.2457(6)	0.008(1)
O3	0.3181(8)	0.7890(8)	0.0510(6)	0.008(1)
Sm_2LiIrO_6				
Sm	0.4818(1)	0.0726(1)	0.2517(1)	0.006(1)
Li	0	0	0	0.008
Ir	1/2	1/2	0	0.004(1)
O1	0.1995(16)	0.3150(16)	0.0482(12)	0.008(2)
O2	0.6026(16)	0.4668(15)	0.2438(12)	0.008(2)
O3	0.3225(18)	0.7910(17)	0.0545(12)	0.010(2)
Eu_2LiIrO_6				
Eu	0.4809(1)	0.0748(1)	0.2515(1)	0.006(1)

Table 2 (*continued*)

	x	*y*	*z*	U_{eq}
Li	0	0	0	0.019(8)
Ir	1/2	1/2	0	0.004(1)
O1	0.1973(18)	0.3169(17)	0.0503(13)	0.008(2)
O2	0.6070(20)	0.4644(17)	0.2445(13)	0.011(2)
O3	0.3258(19)	0.7924(18)	0.0556(14)	0.011(2)

U_{eq} is defined as one-third of the trace of the orthogonalized U_{ij} tensor.

Table 3
Selected interatomic distances (Å), bond angles (deg) and tolerance factors for La_2LiIrO_6, Pr_2LiIrO_6, Nd_2LiIrO_6, Sm_2LiIrO_6, Eu_2LiIrO_6

	La_2LiIrO_6	Pr_2LiIrO_6	Nd_2LiIrO_6	Sm_2LiIrO_6	Eu_2LiIrO_6
Ln–O(2)	2.428(7)	2.368(6)	2.354(4)	2.315(9)	2.297(10)
Ln–O(3)	2.445(7)	2.382(7)	2.374(4)	2.344(9)	2.330(10)
Ln–O(1)	2.445(7)	2.409(6)	2.392(4)	2.358(9)	2.342(10)
Ln–O(2)	2.515(6)	2.421(6)	2.401(4)	2.367(10)	2.349(10)
Ln–O(1)	2.655(7)	2.603(6)	2.586(5)	2.544(10)	2.547(10)
Ln–O(3)	2.661(6)	2.623(7)	2.597(4)	2.573(9)	2.555(10)
Ln–O(1)	2.740(6)	2.666(7)	2.650(4)	2.623(9)	2.614(10)
Ln–O(3)	2.751(7)	2.702(6)	2.702(5)	2.686(9)	2.681(10)
Li–O (× 2)	2.056(7)	2.039(7)	2.035(5)	2.045(9)	2.045(10)
Li–O (× 2)	2.093(6)	2.137(7)	2.131(4)	2.135(9)	2.139(10)
Li–O (× 2)	2.097(6)	2.141(6)	2.143(4)	2.147(10)	2.152(10)
Ir–O (× 2)	1.964(6)	1.964(7)	1.962(4)	1.947(9)	1.951(10)
Ir–O (× 2)	1.966(6)	1.964(6)	1.972(4)	1.970(9)	1.973(10)
Ir–O (× 2)	1.969(6)	1.964(7)	1.977(4)	1.971(10)	1.975(10)
Ir–O–Li	154.3(4)	149.3(4)	148.2(2)	146.8(5)	145.5(5)
Ir–O–Li	154.9(4)	150.2(3)	149.1(2)	146.0(5)	144.6(6)
Ir–O–Li	153.4(4)	148.8(3)	147.5(2)	145.6(5)	144.7(5)
t	0.94	0.93[a]	0.92	0.91	0.90[a]

[a]The ionic radii for Pr^{3+} and Eu^{3+} in CN-12 were obtained through a linear fit extrapolation of known lanthanide element values [26].

cell can be considered a measure of the structural distortion. In the case of the title compounds, as expected, the Li–O–Ir angles decrease with decreasing size of the lanthanide cation while, concomitantly, the β angle increases except in the case of Sm_2LiIrO_6 (see Table 3).

During our previous investigation of Ir(V) double perovskite oxides, Ln_2NaIrO_6 (Ln = La, Pr, Nd), we were unable to prepare members of this series containing lanthanides smaller than neodymium. It appears that a Goldschmidt tolerance factor of approximately 0.86 is the lower limit for Ir(V) containing double perovskites of the type Ln_2BIrO_6. The substitution of the smaller Li^+ for Na^+ increases the tolerance factor such that Sm_2LiIrO_6 ($t = 0.91$ vs. 0.85 for Sm_2NaIrO_6) and Eu_2LiIrO_6 ($t = 0.90$ vs. 0.84 for Eu_2NaIrO_6) could now be prepared. Surprisingly, we were unable to synthesize Gd_2LiIrO_6 ($t = 0.89$) [22] although its tolerance factor is greater than that of the isostructural Nd_2NaIrO_6 ($t = 0.86$). Nonetheless, clearly the reduction in the size of the *B*-cation has proven to be an excellent strategy for incorporating smaller lanthanide elements into the double perovskite structure and work is underway to extend this approach to other platinum group metals, such as osmium.

3.2. Magnetic properties

The temperature dependences of the magnetic susceptibility data for Pr_2LiIrO_6, Nd_2LiIrO_6, Sm_2LiIrO_6, and Eu_2LiIrO_6, are shown in Figs. 2–5. The FC and ZFC data overlay in all cases over the temperature range investigated and, hence, only the ZFC data is shown.

It is known that Ir(V) has a nonmagnetic ground state and, therefore, at low temperatures contributes very little to the magnetic susceptibilities [9,10,23] of Pr_2LiIrO_6, Nd_2LiIrO_6, Sm_2LiIrO_6, and Eu_2LiIrO_6, which are dominated by the magnetism of the rare earth cations. At higher temperatures, however, the Ir(V) species does contribute to the susceptibility, which is not negligible for Eu_2LiIrO_6 and important for Sm_2LiIrO_6. Nonetheless, due to the nonmagnetic

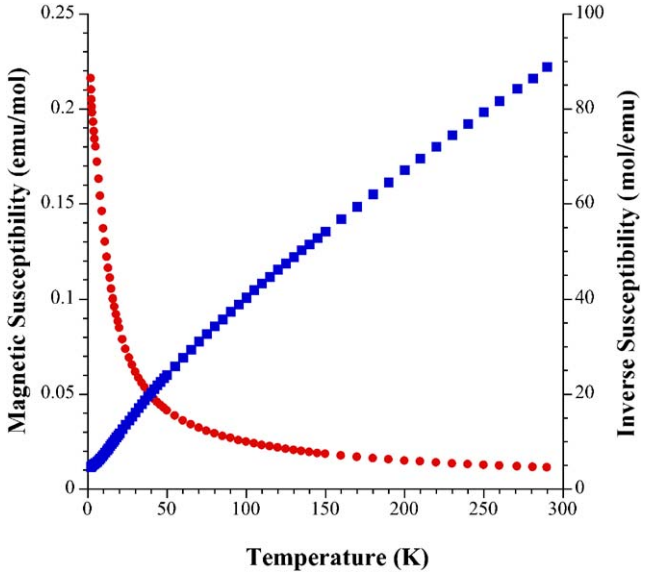

Fig. 2. Temperature dependence of the ZFC magnetic susceptibility (circles) and the inverse susceptibility (squares) of Pr_2LiIrO_6.

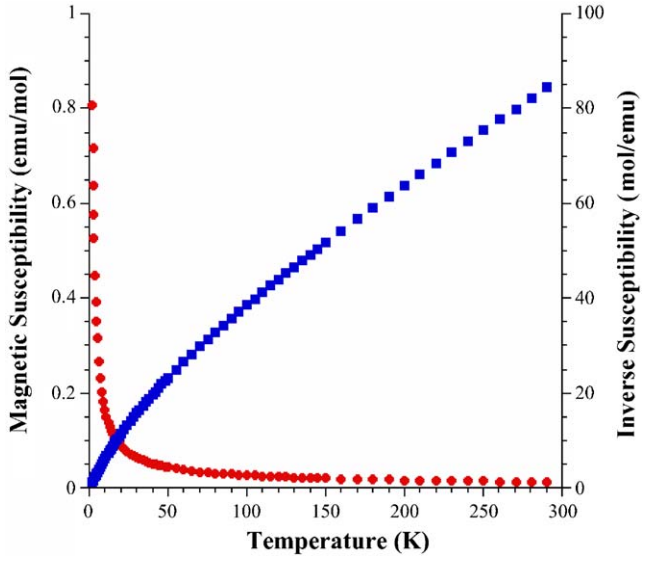

Fig. 3. Temperature dependence of the ZFC magnetic susceptibility (circles) and the inverse susceptibility (squares) of Nd_2LiIrO_6.

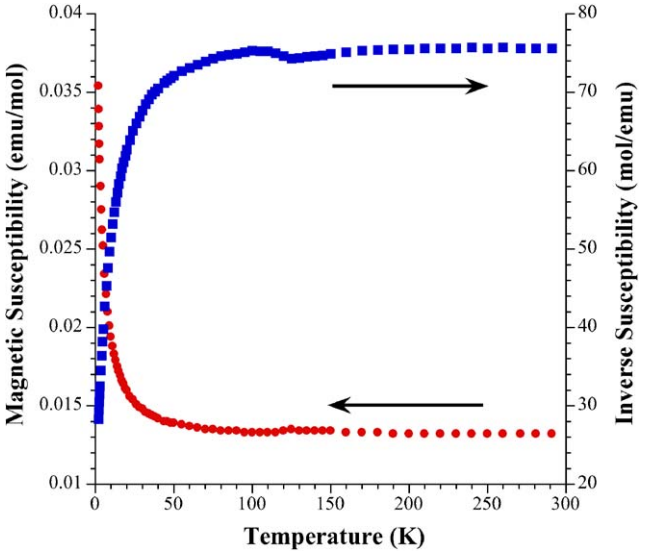

Fig. 4. Temperature dependence of the ZFC magnetic susceptibility (circles) and the inverse susceptibility (squares) of Sm_2LiIrO_6.

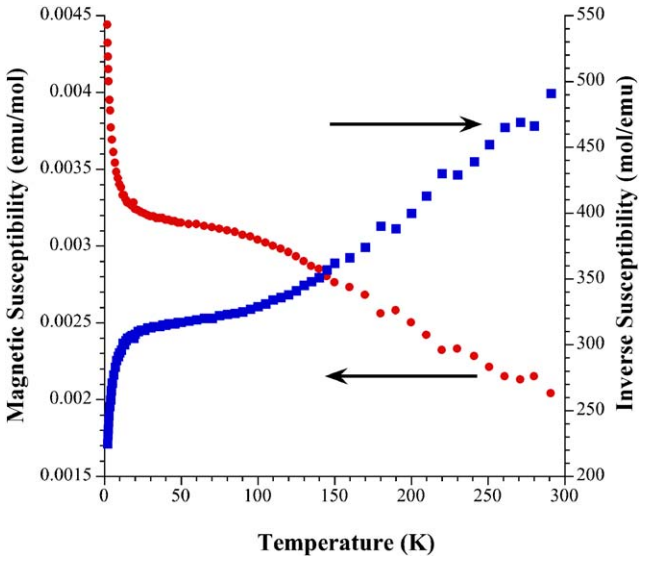

Fig. 5. Temperature dependence of the ZFC magnetic susceptibility (circles) and the inverse susceptibility (squares) of Eu_2LiIrO_6.

ground state of Ir(V), one would not expect to observe magnetic coupling between the rare earth and the iridium cation in these oxides. This is consistent with the observed susceptibility data, which do not give obvious indications of long-range magnetic order in Pr_2LiIrO_6, Nd_2LiIrO_6, Eu_2LiIrO_6, and Sm_2LiIrO_6. Using the inverse susceptibility data from 100 to 300 K, the effective magnetic moments and Weiss constants for Pr_2LiIrO_6 and Nd_2LiIrO_6 were obtained and found to be 5.60 μ_B, $\theta = -57$ K and 5.77 μ_B, $\theta = -59$ K, respectively. These effective moments include contributions from the rare earth cation, and from the iridium (V). The latter contribution is greater at higher temperatures and almost negligible at low temperatures.

The susceptibility data for Sm_2LiIrO_6 and Eu_2LiIrO_6, on the other hand, deviate significantly from Curie–Weiss type behavior, making it impossible to extract a magnetic moment from the inverse susceptibility data. A comparison with magnetic data from the literature shows that the magnetic susceptibility data for Sm_2LiIrO_6, and Eu_2LiIrO_6 are consistent with susceptibility measurements on other samarium and europium containing compounds [24,25].

4. Conclusions

Single crystals of La_2LiIrO_6, Pr_2LiIrO_6, Nd_2LiIrO_6, Sm_2LiIrO_6, and Eu_2LiIrO_6 were grown from molten LiOH/KOH fluxes. The compounds form in the monoclinic distorted double perovskite structure, space group $P2_1/n$ and consists of a 1:1 ordered arrangement of vertex sharing LiO_6 and IrO_6 octahedra. The use of molten hydroxide fluxes continues to be an excellent media for growing oxide single crystals of both lanthanide and platinum group containing metals.

5. Supplementary material

Further details of the crystal structure investigations can be obtained from the Fachinformationszentrum Karlsruhe, 76344 Eggenstein-Leopoldshafen, Germany; fax: +49-7247-808-666; *E-mail address*: crystdata@fiz-karlsruhe.de) on quoting the depository numbers CSD-414149-414152 for Ln_2LiIrO_6 (Ln = Pr, Nd, Sm, Eu) and CSD-414605 for La_2LiIrO_6.

Acknowledgments

This work was supported by the Department of Energy through grant DE-FG02-04ER46122 and the National Science Foundation through grant DMR: 0134156.

References

[1] M. Wakeshima, D. Harada, Y. Hinatsu, J. Alloys Compd. 287 (1999) 130.
[2] P.D. Battle, J.G. Gore, R.C. Hollyman, A.V. Powell, J. Alloys Compd. 218 (1995) 110.
[3] M.J. Davis, S.J. Mugavero III, K.I. Glab, M.D. Smith, H.-C. zur Loye, Solid State Sci. 6 (2004) 413.
[4] M.J. Davis, M.D. Smith, H.-C. zur Loye, Inorg. Chem. 42 (2003) 6980.
[5] W.R. Gemmill, M.D. Smith, H.-C. zur Loye, Inorg. Chem. 43 (2004) 4254.
[6] W.R. Gemmill, M.D. Smith, H.-C. zur Loye, J. Solid State Chem. 177 (2004) 3560.
[7] SAINT+ Version 6.22 and SADABS 6.22 Bruker Analytical X-ray Systems SMART Version 5.625, Inc., Madison, WI, 2001.
[8] G.M. Sheldrick, SHELXTL Version 6.1, Bruker Analytical X-Ray Systems, Inc., Madison, WI, 2000.
[9] A.V. Powell, J.G. Gore, P.D. Battle, J. Alloys Compd. 201 (1993) 73.
[10] K. Hayashi, G. Demazeau, M. Pouchard, P. Hagenmuller, Mater. Res. Bull. 15 (1980) 461.
[11] S.W. Keller, V.A. Carlson, D. Sanford, F. Stenzel, A.M. Stacy, G.H. Kwei, M. Alario-Franco, J. Am. Chem. Soc. 116 (1994) 8070.
[12] H. Lux, Z. Elektrochem. 45 (1939) 303.
[13] H. Flood, T. Forland, Acta Chem. Scand. 1 (1947) 592.
[14] J.L. Luce, A.M. Stacy, Chem. Mater. 9 (1997) 1508.
[15] R.H. Mitchell, Perovskites: Modern and Ancient, Almaz Press, Ontario, 2002.
[16] P.M. Woodward, Acta Crystallogr. B 53 (1997) 44.
[17] P.M. Woodward, Acta Crystallogr. B 53 (1997) 32.
[18] A.M. Glazer, Acta Crystallogr. B 28 (1972) 3384.
[19] S.-J. Kim, M.D. Smith, J. Darriet, H.-C. zur Loye, J. Solid State Chem. 177 (2004) 1493.
[20] J.F. Vente, D.J.W. IJdo, Mater. Res. Bull. 26 (1991) 1255.
[21] K.E. Stitzer, W.R. Gemmill, M.D. Smith, H.-C. zur Loye, J. Solid State Chem. 175 (2003) 39.
[22] Large crystals of the phase Li_8IrO_6 (pdf 78-0341) were obtained in our attempts to synthesize Gd_2LiIrO_6.
[23] M. Walewski, B. Buffat, G. Demazeau, F. Wagner, M. Pouchard, P. Hagenmuller, Mater. Res. Bull. 18 (1983) 881.
[24] K. Koteswara Rao, M. Vithal, D. Ravinder, J. Magn. Magn. Mater. 253 (2002) 65.
[25] L. Thompson, J. Legendziewicz, J. Cybinska, L. Pan, W. Brennessel, J. Alloys Compd. 341 (2002) 312.
[26] R.D. Shannon, Acta Crystallogr. A 32 (1976) 751.